Protein purification of Mcfp-1. Mcfp-1 was purified as previously described with some modifications.[1] The mussels were harvested off Goleta Pier, (Santa Barbara, Ca.), and held in circulation tanks. The mussels were shucked and the foot was severed from the body and frozen to -70 ^{0}C before fileting off the pigmented epithelium. Approximately 50 prepared feet were homoginized in four equivalents (w/v) of 5% acetic acid (v/v), 10 μM leupeptin, 10 μM pepstatin, and 1mM EDTA in a glass tissue grinder (Kontes, Vineland, NJ) on ice and centrifuged at 20,00 X g, 4 ^{0}C for 40 min. The supernatant was acidified with 70% perchloric acid to a final concentration of 1.5% (v/v). After centrifugation at 20,000 X g, 4 ^{0}C for 40 min, the supernatant was dialyzed 4 X 4L of 5% acetic acid (v/v) for four hours and overnight with in Spectrum Industries 1,000 kDa molecular weight cutoff dialysis tubing (Los Angeles, Ca) before freeze drying. The lyophilized protein was resuspended in 200 μl of 5% acetic acid (v/v) and 50 μl aliquots were run over a Shodex KW-803 size exclusion column (5 μm, 8 x 300 mm) (New York, NY). Fractions were monitored at 280 nm and those positive for protein were subjected to acid-urea polyacrylamide gel electrophoresis (7.5% acrylamide and 0.2% *N*,*N*_-methylenebisacrylamide) containing 5% acetic acid and 8 M urea.[2] After electrophoresis, gels were stained with Sigma-Aldrich Coomassie Blue R-250 (Brooklyn, NY). Pure mcfp-1 fractions were pooled and aliquoted before freeze-drying and stored at -70 ^{0}C for future use.

Recombinant Mefp-1 and enzymatic modification. rMefp-1 without Dopa was generously donated by Dr. Dong Soo Hwang (Pohang University of Science and Technology, Korea) and prepared as in Zheng et al.[3] Dopa enzymatic modification:[4] The rMefp-1 (1 mg) was dissolved in 1 ml pH 6.5, 10 mM borate, 0.05 M phosphate-ascorbate buffer, in an Eppendorf microfuge tube. Mushroom tyrosinase (3000 U/mg) was from Aldrich-Sigma and all other reagents were of analytical grade. After adding mushroom tyrosinase (0.3 mg), the tube was shaken for 4 hrs at ambient room temperature and pressure. The reaction was stopped by adding 40 μl glacial acetic acid, and the resulting product was subjected to reverse phase HPLC column, eluted with a linear gradient of aqueous acetonitrile. Eluant was monitored continuously at 230 and 280 nm, and 0.33 ml fractions containing peptides were pooled and freeze-dried. Sample purity and hydroxylation were assessed by amino acid analysis, and MALDI time-of-flight mass spectrometry.

Purification of Mefp-5. Mefp-5 was purified as described previously.[5] rMfp-5 was a generous gift from Professor H.J. Cha (Pohang University of Science and Technology, Korea) prepared as in Choi et al.[6] All proteins were checked for purity by acid urea gels, MALDI and amino acid analysis.

Purification of Mcfp-3F and Mcfp-3S. Mfp-3F and Mfp-3S were purified from the plaques of the California mussels, *Mytilus californianus* respectively as described elsewhere.[7] About 1000 accumulated plaques were thawed and homogenized in a small volume (5 ml/200 plaques) of 5% acetic acid (v/v) containing 8 M urea on ice using a small hand-held tissue grinder (Kontes, Vineland, NJ). The homogenate

was centrifuged for 30 min at 20,000 × g and 4 °C. The soluble acetic acid/urea plaque extracts were subjected to reverse phase HPLC using a 260 × 7-mm RP-300 Aquapore (Applied Biosciences Inc., Foster City, CA) , eluted with a linear gradient of aqueous acetonitrile. Eluant was monitored continuously at 230 and 280 nm, and 1-ml fractions containing Mfp-3F and Mfp-3S were pooled and freeze-dried, injected into Shodex-803 column (5 μm, 8 × 300 mm), which was equilibrated and eluted with 5% acetic acid in 0.1% trifluoroacetic acid. Eluant was monitored at 280 nm. Sample purity was assessed by acid urea-PAGE, amino acid analysis, and MALDI time-of-flight mass spectrometry. Fractions with pure Mfp-3F and Mfp-3S were freeze-dried and re-dissolved in buffers for further studies.

Sample preparation. For the polystyrene and silica spin labeling, 10 mM, 250 μL Tempo-4-carboxylate (Sigma-Aldrich) dissolved in 0.2 M MES buffer (Sigma Aldrich) at pH 3.0 was mixed with 100 μL amine-modified polystyrene bead (Sigma Aldrich) and 100 uL 3-aminopropyl functionalized silica (Sigma Aldrich), respectively in the presence of a cross-linker, 38 mM, 90 μL 1-ethyl-3-(3-dimethylaminopropyl) carbodiimide (EDC) (Thermo Scientific) for one day at room temperature. EDC and free Tempo-4-carboxylate were washed out several times with MES buffer, pH 3.0. The diameter of spin labeled polystyrene beads (SLPS) and silica beads ($SLSiO_2$) were measured with dynamic light scattering (DLS). The measured SLPS and $SLSiO_2$ beads diameters are 63 nm and 30 nm. The beads are neutral in charge, with a zeta potential of approximately 0 mV.

7.5 mg/mL Mfps, poly-L-lysine, 4.5 kDa polyethylene glycol (PEG), bovine serum albumin (BSA) and 90 mg/mL BSA were dissolved in MES buffer, pH 3.0 and mixed with SLPS and $SLSiO_2$ solution with a volume ratio of 1:2, respectively. P188 was a generous gift of BASF (Wyandotte, MI).

ESR and ODNP Experiments. A 3.2 μL sample was loaded in a 0.6 mm I.D. quartz capillary tube (fiber Optic Center Inc., New Bedford, MA) and sealed at both ends with beewax. The capillary was mounted on a home-built NMR probe with a U-shaped NMR coil connected to a Bruker Avance spectrometer and held within the TE_{102} microwave cavity. Continuous wave ESR spectra were measured on a Bruker (Billerica, MA) X-band EMX ESR spectrometer with a rectangular TE_{102} cavity at 6 mW incident power, by using a field modulation 0.7 G at room temperature. ^1H ODNP measurements were done at a 0.35 T electromagnet at 14.8 MHz ^1H Larmor frequency and at 9.8 GHz electron Larmor frequency under airflow in order to minimize sample heating upon microwave irridation at room temperature. During ODNP experiments, the center field of nitroxide hyperfine transition lines was pumping continuously by microwave irradiation at 9.8 GHz, while ^1H NMR signal was recorded. T_1 and T_{10} spin-lattice relaxation times (with and without spin label, respectively) were measured by inversion recovery experiments in order to determine the leakage factor. The ^1H NMR signal enhancement of water was recorded as a function of increasing microwave power that was controlled by a home-built X-band microwave amplifier.

The detailed description of ODNP can be found in the literature.[8-10] Here, we only provide a brief summary of the ODNP theory. ^{1}H ODNP relies on the polarization transfer from the electron spin of nitroxide radicals to the ^{1}H of water via cross relaxation induced by the saturation of electron spin transitions through continuous wave (cw) microwave irradiation. The maximum ^{1}H NMR signal enhancement E_{max} is given by[8,11]

$$E_{\max} = E(P \to \infty) = 1 - \rho f s_{\max} \frac{|\gamma_s|}{\gamma_I} \qquad (1)$$

where ρ is the coupling factor, a key parameter for determining dynamics, f is the leakage factor, s_{max} is the maximum electron spin saturation factor, γ_s *and* γ_I are the gyromagnetic ratios of the electron and proton spins, given by $|\gamma_s|/\gamma_I = 658$. E_{max} can be measured by obtaining enhanced ^{1}H NMR signal of water as a function of microwave power (P) and extrapolating he value to infinite power. The leakage factor can be determined experimentally by measuring the longitudinal relaxation times of samples in the presence (T_1) and absence (T_{10}) of electron spin, using the relation $f = 1 - T_1/T_{1,0}$. Unlike the coupling and saturation factors, the leakage factor critically depends on the spin label concentration. To obtain the s_{max}, full saturation of all ESR transitions, and so complete exchange of the hyperfine lines of the nitroxide radical has to be achieved. For nitroxide radicals tethered to slow tumbling macromolecules, the condition of $s_{max} \approx 1$ is fulfilled.[11] The coupling factor is determined from Eq. S1 because other parameters in eq. S1 are now known. The coupling between water proton and electron spin is dominated by dipolar interaction, and the fluctuation of electron-proton dipolar interaction due to translational diffusion dynamics can be expressed with a single correlation time. Thus, a single spectral density function $J(\omega,\tau)$ can describe the interaction and taken together, ρ is given by[12]

$$\rho = \frac{6J(\omega_s + \omega_I, \tau) - J(\omega_s - \omega_I, \tau)}{6J(\omega_s + \omega_I, \tau) + 3J(\omega_I, \tau) + J(\omega_s - \omega_I, \tau)} \qquad (2)$$

where ω_s is the electron Larmor frequency, ω_I is the nuclear Larmor frequency, and τ is the translational correlation time between the water proton and electron, at the given distance of closest approach between the two spins. Here, we extract the translational correlation time by employing the force-free hard sphere dynamic model developed by Hwang and Freed.[13]

The new ODNP analysis method to separate and evaluate the fast (ps) scale water motion, k_σ, from slow (ns) scale motion, k_{low}, is described in Hussain et. al.[10], namely:

$$k_\sigma = \frac{1 - E_{\max}}{C_{SL} T_1} \left(\frac{\gamma_I}{\gamma_s} \right)$$
$$k_\rho = \frac{T_1^{-1} - T_{1,0}^{-1}}{C_{SL}} \qquad (3)$$
$$k_{low} = \frac{5}{3} k_\rho - \frac{7}{3} k_\sigma$$

where k_σ and k_ρ are relaxivity rates having units of $s^{-1}M^{-1}$, both describing relaxation rates that are proportional to the concentration of the spin label, C_{SL}. The k_σ depends on the transition probabilities between spin states have characteristic frequencies at the ESR transition (10 GHz), while the k_ρ depends on also the transition probability between spin states have characteristic frequencies at the NMR frequency (15 MHz). Therefore, k_σ contains only fast dynamics information while k_ρ also contains contributions from slow motions. The k_{low} can be obtained after subtract the fast motion contribution from k_ρ.

Quartz Crystal Microbalance with Dissipation (QCM-D). Monitoring. Silica sensors (Biolin Scientific Inc.) were cleaned by rinsing with 2% SDS, acetone, ethanol and Milli-Q water respectively. The silica sensors were further cleaned by UV/ozone plasma for 15 min. The QCM-D measurements were carried out in a Q-Sense E4 system using an open cell in static solution. Samples were deposited into the open cell using a 20-P pipette man. Changes in resonance frequency (ΔF) and dissipation (ΔD) of the silica quartz crystal were recorded to determine the amount of protein adsorbing to the sensor and the viscoelastic properties of the protein film. The silica crystal was excited at its fundamental frequency of approximately 5 MHz, and changes can be observed at the fundamental frequency (n=1) in addition to overtone frequencies (n=3, 5, 7 and 11). Readings were taken from overtone frequencies n=7 and 9.

Supporting Table 1 | Mussel foot proteins.

Protein	Species	Amino acid numbers	Mass (kDa)	pI	Dopa (mol%)	Hydrophathy (per AA)
Mfp-1	Mc	732	85.0		20	+0.16
rMfp-1	Me	120	13.6		20	+0.14
rMfp-1 w/o Dopa	Me	120	13.6		0	+0.07
Mfp-3S	Mc	45	5.3	8.3	8	-0.49
Mfp-3F	Mc	42	5.2	10.2	17	+0.14
Mfp-5	Me	73	8.5	9.0	28	+0.20
rMfp-5 w/o Dopa	Me	73	8.5		0	+0.07

Mc denotes Mytilus californianus, Me denotes Mytilus edulis.[14]

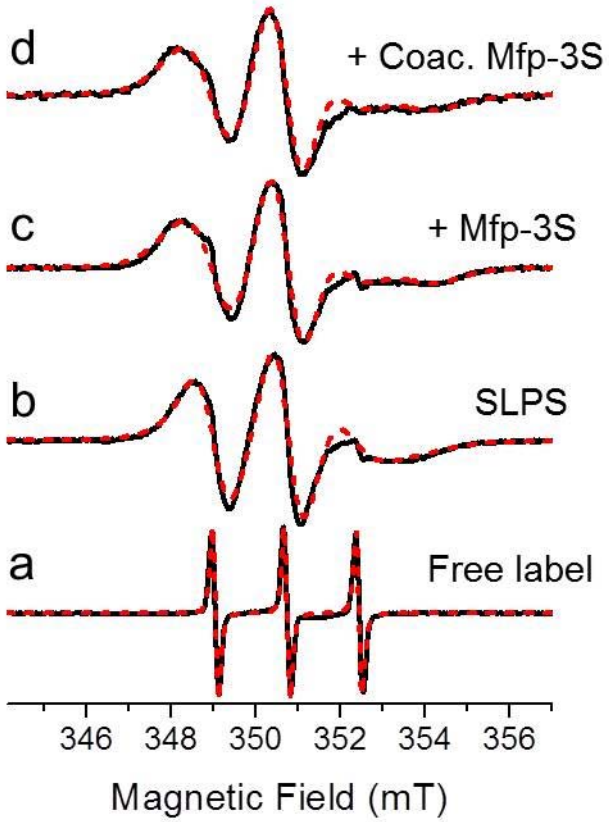

Supporting Figure 1. CW ESR spectra of free and bound spin radicals (black) and their simulations (red). **(a)** Dissolved free Tempo-4-carboxylate in MES buffer, τ = 20 ps. (**b)** Spin labeled polystyrene beads, τ = 4.2 ns. **(c)** After addition of (2.5 mg/mL) Mfp-3S to the SLPS, τ = 5.7 ns. (**d)** After addition of (2.5 mg/mL) coacervated Mfp-3S to the SLPS, τ = 5.7 ns.

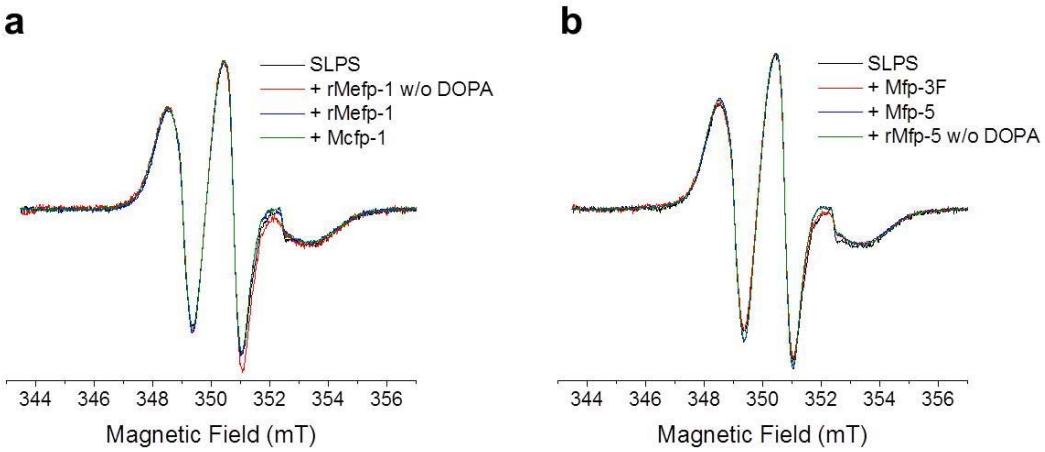

Supporting Figure 2. CW ESR spectra of SLPS and after addition of (2.5 mg/mL) Mfps. ESR lineshape does not change after addition of **(a)** Mcfp-1, rMefp-1 and rMefp-1 without Dopa, and (**b)** Mfp-3F, Mfp-5 and rMfp-5 without Dopa.

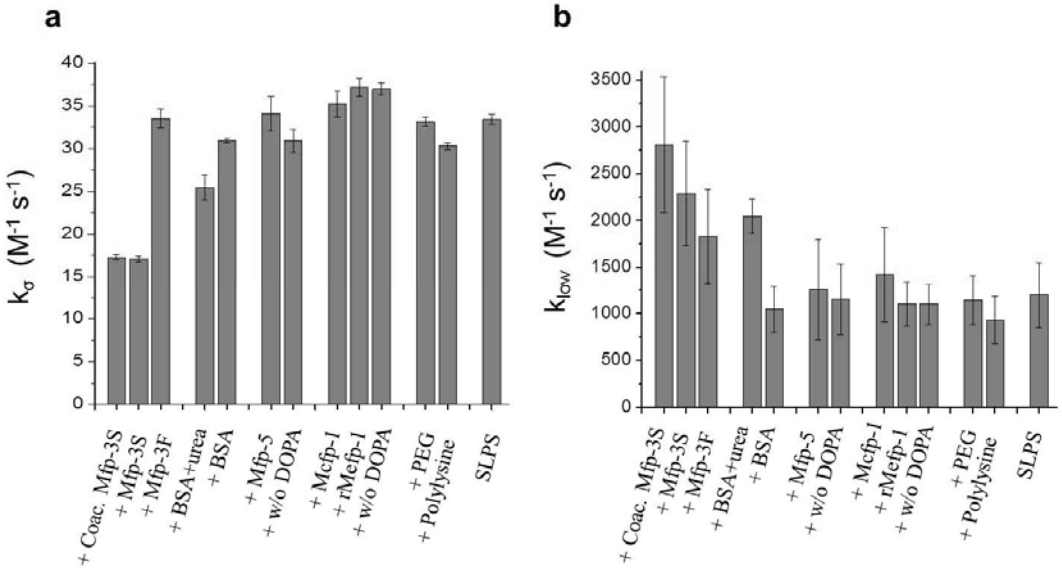

Supporting Figure 3. ODNP parameters of SLPS and after addition of proteins and polymers in MES buffer, pH 3.0 and coacervated Mfp-3S in MES buffer, pH 5.5. **(a)** Fast water dynamics (k_σ) is slower after addition of (2.5 mg/mL) coacervated and noncoacervated Mfp-3S, and also 5 M urea induced BSA compared to the k_σ of SLPS. Addition of (2.5 mg/mL) Mfp-3F, BSA, Mfp-5, Mfp-5 without Dopa, Mcfp-1, rMefp-1, rMefp-1 without Dopa, PEG and Polylysine do not change the k_σ value of SLPS. **(b)** Slow water dynamics (k_{low}) increases only after addition of coacervated and noncoacervated (2.5 mg/mL) Mfp-3S, Mfp-3F and also urea induced BSA compared to the k_{low} of SLPS.

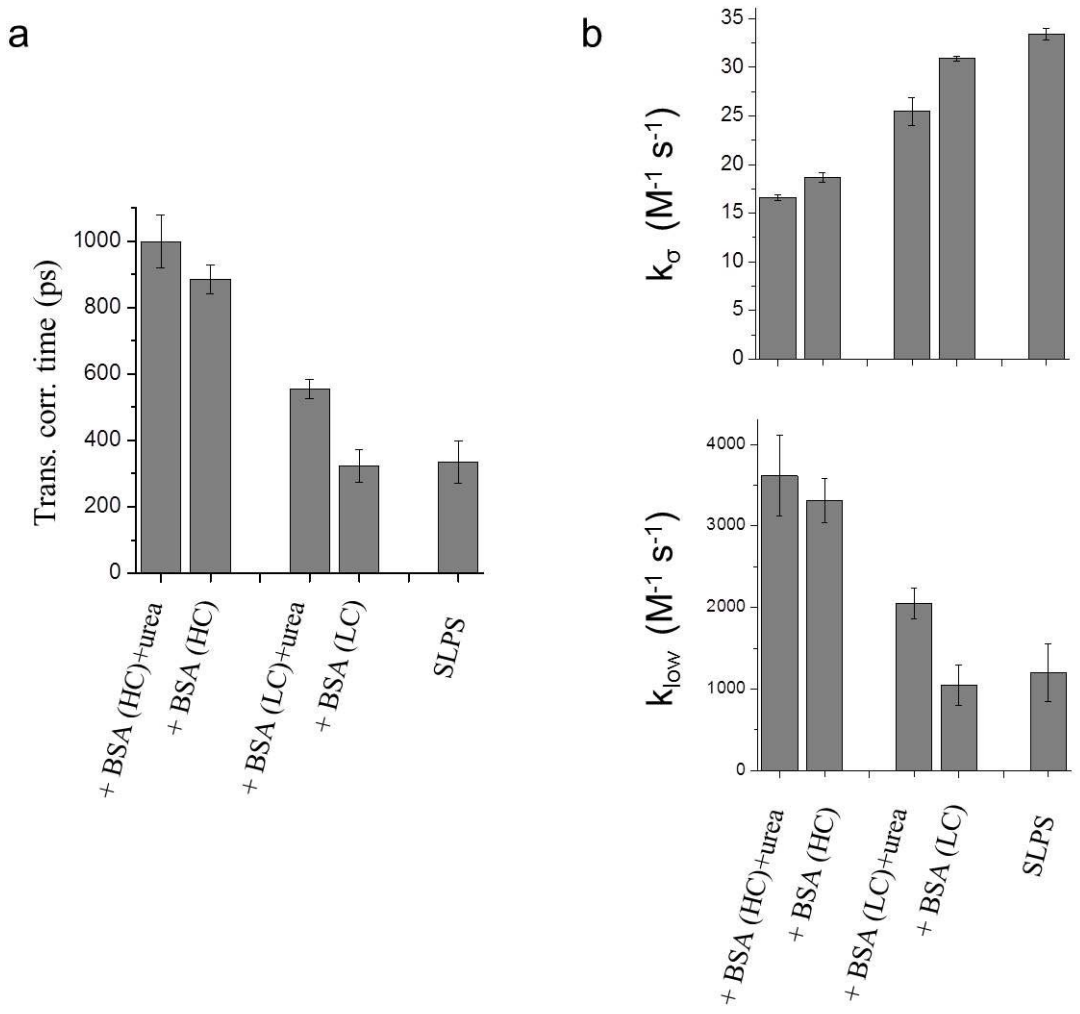

Supporting Figure 4. ODNP parameters of SLPS and after addition of BSA. **(a)** Translational correlation time ($\tau_{surface\text{-}water}$), **(b)** fast water dynamics (k_σ) and slow water dynamics (k_{low}) of SLPS and after addition of low concentration (2.5 mg/mL) and high concentration (30 mg/mL) of BSA with and without 5M urea. Hydration water dynamics slows down with increasing BSA concentration and also addition of urea.

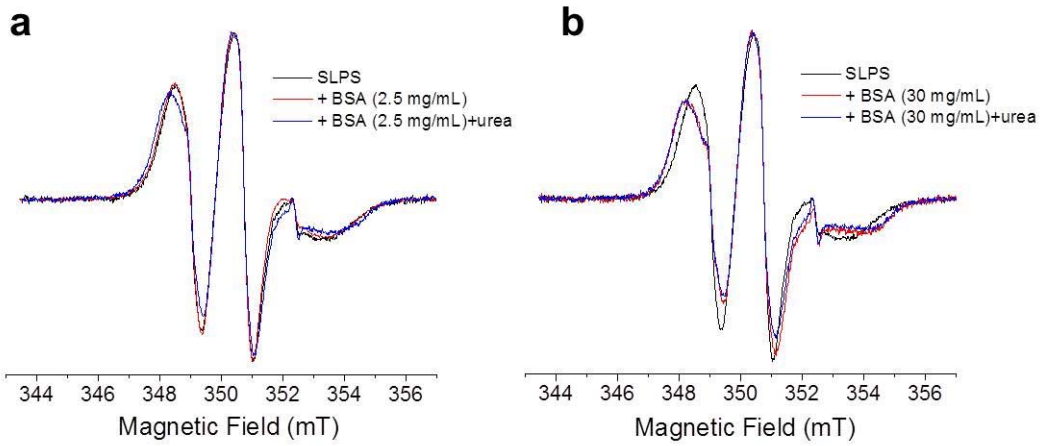

Supporting Figure 5. CW ESR spectra of SLPS and after addition of BSA. (**a)** Addition of 2.5 mg/mL BSA does not change the ESR line shape of SLPS but addition of 5M urea induced BSA restricts the motion. **(b)** Addition of 30 mg/mL BSA slows down the motion of spin labels on the PS surface more than addition of 2.5 mg/mL BSA. ESR spectrum of SLPS after addition of 5 M urea induced BSA (30 mg/mL) is very similar to the ESR spectrum of SLPS after addition of BSA (30 mg/mL).

It is of interest to compare the results with Mfps to the behavior of BSA, as BSA is frequently used as a "standard protein", and also as a blocking agent to prevent nonspecific hydrophobic binding of antigens and antibodies to the undesired surface. At pH 3, BSA is partially folded with 40% of its initial α-helix lost[15]—the SLPS surface water diffusivity remains unaltered under this condition. However, when BSA is unfolded (by adding urea at 5 mM at pH 3), its addition to the solution moderately slows the hydration dynamics on the SLPS surface from 335 ps to 555 ps (**Fig. 2b)**, which implies that initially-hidden hydrophobic segments become accessible to facilitate interaction with the SLPS surface. Still, Mfp-3S interacts much more intimately with SLPS surfaces than unfolded BSA, and comparably in the presence of 12-fold concentrated BSA with resulting τ of 885 ps and 998 ps with and w/o 5 M urea, respectively (**Supporting Fig. 4)**. The cw ESR lineshapes (**Supporting Fig. 5**) consistently show increased immobilization of the spin labels with increasing BSA concentration, confirming increased protein adsorption.

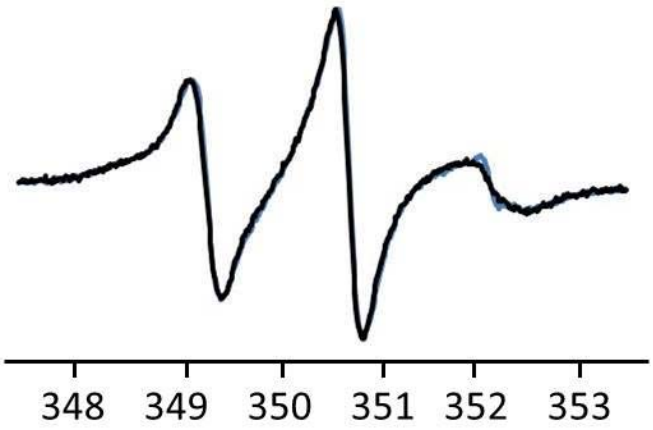

Supporting Figure 6. CW ESR spectra of spin labeled silica before (black) and after addition of (2.5 mg/mL) Mfp-3S (blue). $\tau = 2.5$ ns.

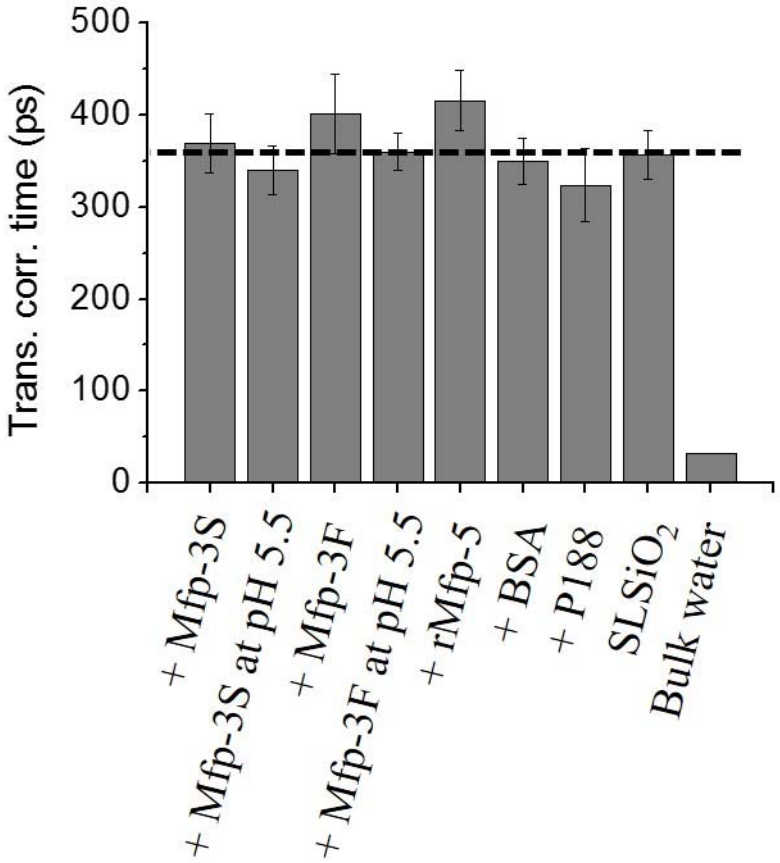

Supporting Figure 7. Translational correlation time ($\tau_{surface\text{-}water}$) of hydration water at surface of spin labeled silica ($SLSiO_2$) before and after addition of (2.5 mg/mL) Mfp-3S (pH 3.0 and 5.5), Mfp-3F (pH 3.0 and 5.5), rMfp-5 (pH 3.0), 5 mg/mL BSA (pH 3.0), 0.84 mg/mL P188 (pH 3.0) in MES buffer. τ_{bulk} value is 33 ps, measured by ODNP using a nitroxide radical in water.[16,17] Error bar represents the standard deviation. The horizantal dashed line marks the reference τ value of the bare $SLSiO_2$ surface. None of the proteins and polymers bound to the $SLSiO_2$ surface.

For spin labeled silica ($SLSiO_2$), cw ESR line-shape analysis shows the presence of a single population of slow and anisotropically moving spin labels with an average rotational correlation time of $\tau_R = 2.5$ ns, which is faster than the rotational correlation time of spin labels on the PS beads (4.2 ns). This can be explained by having the longer label side chain of silica. The ODNP-derived $\tau_{surface\text{-}water}$ on spin labeled silica surfaces was found to be 357 ps which is very similar to $\tau_{surface\text{-}water}$ of SLPS (335 ps). In the presence of native Mfp-3S, Mfp-3F at pH 3.0 and 5.5 or rMfp-5, BSA, the hydrophilic polymer of P188 (known as a membrane sealant) at pH 3.0 the $\tau_{surface\text{-}water}$ values and their ESR spectra do not change beyond the margin of error, signifying that none are achieving intimacy with the silica surfaces.

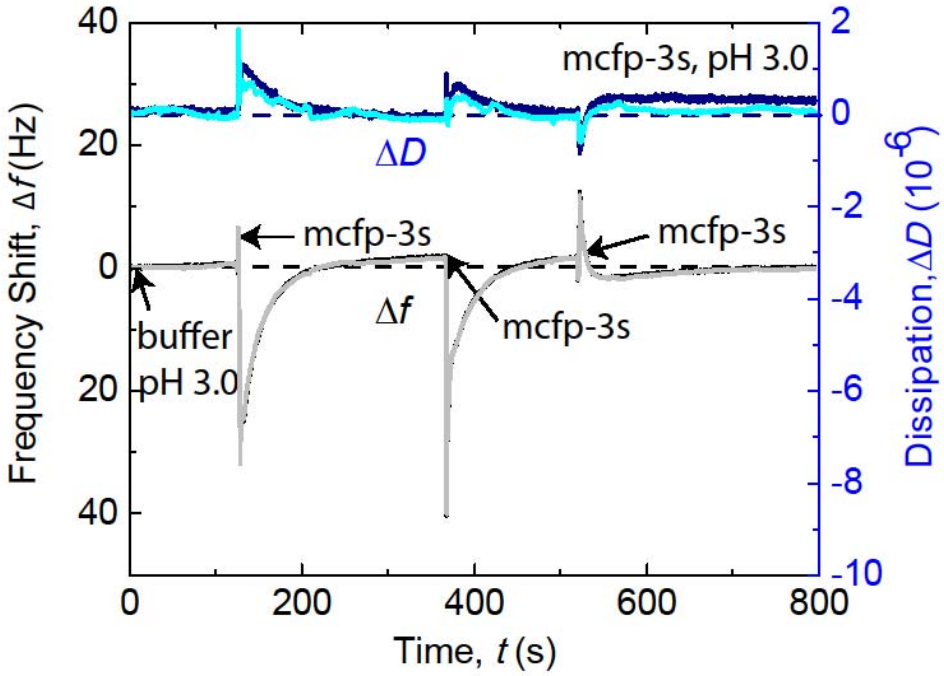

Supporting Figure 8. Frequency and dissipation change upon addition of (20 µg/mL) Mfp-3S to a silica surface. In this three-step adsorption, Mfp-3S was deposited onto a silica surface at pH 3.0 using a static cell. Buffer addition of pH 3 (100 µL) and Mfp-3S additions (20 µL, 20 µL and 60 µL) were added as indicated in the figures.

Protein adsorption experiments in a Quartz Crystal Microbalance (QCM-D) indicated that Mfp-3S (20 µg/mL) did not adsorbed to a silica surface at pH 3.0 and high salt (250 mM KNO_3) (Fig. S8). The change in dissipation of the quartz crystal was negligible after each addition of Mfp-3S, indicating that the Mfp-3 did not adsorb to the surface.

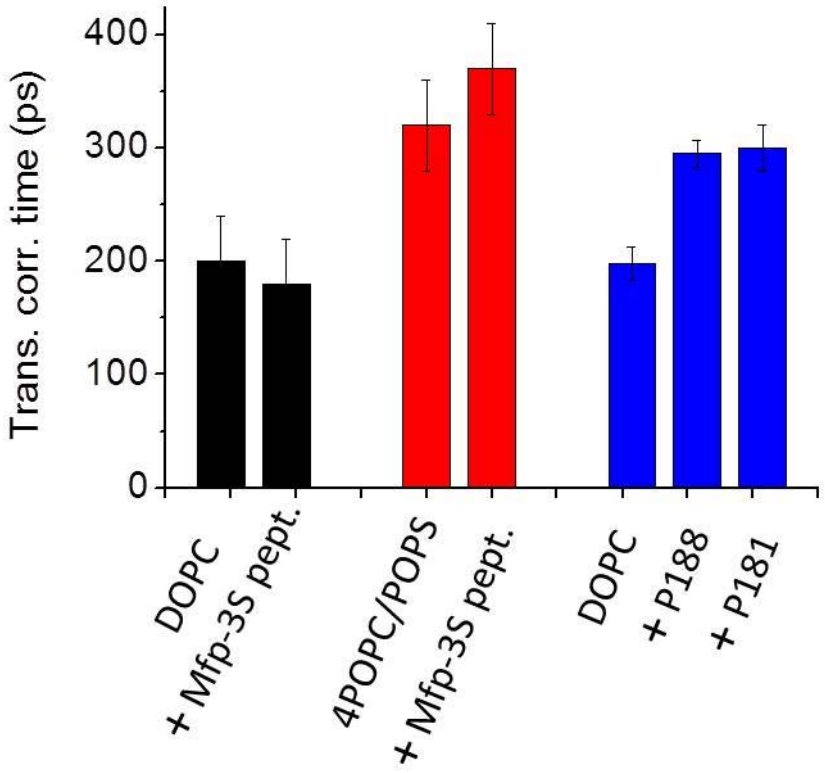

Supporting Figure 9. Translational correlation time ($\tau_{surface\text{-}water}$) of hydration water at the surface of spin labeled liposomes, freely suspended in solution, composed of DOPC and POPC/POPS bilayer membranes before and after addition of (2.5 mg/mL) Mfp-3S peptide and the PEO-PPO copolymer (P188, 0.92 mg/mL, and P181, 0.07 mg/mL). Translational correlation time ($\tau_{surface\text{-}water}$) of surface hydration dynamics of DOPC and after addition of Mfp-3S peptide (black), $\tau_{surface\text{-}water}$ of 4POPC/POPS and after addition of Mfp-3S peptide (red) in MES buffer at pH 3.0. $\tau_{surface\text{-}water}$ of DOPC and after addition of P188 and P181 (blue) in water (adapted from Ref.18). Error bar represents the standard deviation. Similar to the $SLSiO_2$ surface, the hydrophilic surfaces DOPC and 4POPC/POPS did not offer measurable spontaneous adhesion of the Mfp-3S peptide.

Phospholipid DOPC (1,2-dioleoyl-sn-glycero-3-phosphocholine) and spin labeled phospholipids PC Tempo (1,2-dioleoyl-sn-glycero-3-phospho (tempo) choline) were purchased from Avanti Polar Lipids Inc. (Alabaster, AL). 32 mM lipid solution with 0.64 mM spin label solution in 200 mM MES buffer at pH 3.0 was prepared as described earlier.[18]

Mfp-3S peptide with a sequence of GYDGYNWPYGYNGYRYGWNKGWNGY was prepared in Waite Lab. Addition of Mfp-3S peptide at pH 3 also resulted in significant retardation of PS surface water but not

that of silica surface water (not shown). 32 mM lipid concentration with 0.64 mM spin label solution was prepared with POPC (1-palmitoyl-2-oleoyl-sn-glycero-3-phosphocholine, spin labeled POPC (1-palmitoyl-2-oleoyl-sn-glycero-3-phospho (tempo) choline) and POPS (1-palmitoyl-2-oleoyl-sn-glycero-3-phospho serine) were purchased from Avanti and prepared as described earlier.[19]

In the presence of Mfp-3S peptide, the $\tau_{surface\text{-}water}$ of DOPC and POPC/POPS do not change beyond the margin of error, showing that Mfp-3S peptide does not bind to DOPC and POPC/POPS.

P188 is the most hydrophilic polaxamer and known as a membrane sealant. Another polaxamer P181 is the most hydrophobic polaxamer and known as membrane permeabilizer. These two polaxamers retarded DOPC membrane hydration dynamics shown with ODNP.[18]

References

1. Zhao, H.; Waite, J. H. *J. Biol. Chem*. **281**, 26150, 2006.

2. Waite, J. H.; Benedict, C. V. *Methods Enzymol.* **107**, 397, 1984.

3. Zeng, H.; Hwang, D.S.; Israelachvili, J.N.; Waite, J. H. *Proc. Natl. Acad. Sci. USA* **107,** 12850, 2010.

4. Taylor, S.W. *Anal Biochem*, **302**, 70, 2002.

5. Danner, W. E.; Kan, Y.; Hammer, U. M.; Israelachvili, J. N.; Waite, J. H. *Biochemistry* **51**, 6511, 2012.

6. Choi, Y.S. *et al. Biofouling* **27,** 729, 2011.

7. Zhao, H.; Robertson, N. B.; Jewhurst, S. A.; Waite, J. H. *J. Biol. Chem*. **281**, 11090, 2006.

8. Armstrong, B. D.; Han, S. *J. Am. Chem. Soc*. **131**, 4641, 2009.

9. Franck, J. M.; Pavlova, A.; Han, S. *Prog. Nucl. Magn. Reson*. DOI: 10.1016/j.pnmrs.2013.06.001 (2013).

10. Hussain, S.; Franck, J. M.; Han, S. *Angew. Chem. Int. Ed*. **52**, 1953, 2013.

11.Armstrong, B.D.; Han, S. *J. Chem. Phys.* **127**, 104508, 2007.

12. Hausser, K.H.; Stehlik, D. *Adv. Magn. Reson*. **3**, 79, 1968.

13. Hwang, L. P.; Freed, J. H. *J. Chem. Phys*. **63**, 4017, 1975.

14. Lee, B.P.; Messersmith, P.B.; Israelachvili, J.N.; Waite, J.H. *Annu. Rev. Mater. Res*. **41**, 99, 2011.

15. El Kadi, N.; Tauilier N.; Le Huerou, J.Y.; Gindre, M.; Urbach, W.; Nwigwe, I.; Kahn, P.C.; Waks, M. *Biophys. J*. **91**, 3397, 2006.

16. Bennati, M.; Luchinat, C.; Parigi, G.; Türke, M.T. *Phys. Chem. Chem. Phys.* **12**, 5902, 2010.

17. Franck, J. M.; Pavlova, A.; Scott, J. A.; Han, S. *Prog. Nucl. Magn. Reson*. **74**, 33, 2013**.**

18. Cheng, C.; Wang, J.; Kausik, R.; Lee, K. C.; Han, S. *Biomacromolecules* **13**, 2624, **2012**.

19. Song, J.; Franck, J.; Pincus, P.; Kim, M. W.; Han, S. *J. Am. Chem. Soc.* **136**, 2642, 2014.